Thermal Properties of $[M_{10}Se_4(SePh)_{12}(PR_3)_4]$ (M = Zn, Cd, Hg) Cluster Molecules – Synthesis and Structure of $[Cd_{32}Se_{14}(SePh)_{36}(L)_4]$; L = $OPPh_3$, OC_4H_8

Andreas Eichhöfer*[a]

Keywords: Cluster compounds / Cadmium / Selenium / X-ray structure analysis / Thermogravimetric analysis

A series of four different M_{10} selenide cluster molecules of the general formula $[M_{10}Se_4(SePh)_{12}(PR_3)_4]$ (M = Zn, Cd, Hg; R = organic group) have been synthesized by the reaction of metal chlorides MCl_2 (M = Zn, Cd, Hg) with phosphanes PR_3, $Se(SiMe_3)_2$ and $PhSeSiMe_3$ in organic solvents. The investigations of the thermal properties by thermogravimetric analysis (TGA) reveal that $[Zn_{10}Se_4(SePh)_{12}(PnPr_2Ph)_4]$, $[Cd_{10}Se_4(SePh)_{12}(PEt_3)_4]$, $[Cd_{10}Se_4(SePh)_{12}(PnPr_3)_4]$ and $[Hg_{10}Se_4(SePh)_{12}(PnPrPh_2)_4]$ form the corresponding bulk chalcogenides in mainly two- or three-step processes. From the intermediate product of the first step of the vacuum thermolysis of $[Cd_{10}Se_4(SePh)_{12}(PnPr_3)_4]$ we were able to obtain in solution the larger cluster molecule $[Cd_{32}Se_{14}(SePh)_{36}(OC_4H_8)_4]$ and upon addition of $OPPh_3$ its homologue $[Cd_{32}Se_{14}(SePh)_{36}(OPPh_3)_4]$. The structures of both molecules have been determined by single-crystal XRD. Obviously, the smaller Cd_{10} cluster grows upon thermal treatment in the solid state to form larger cluster cores. However, optical spectra and dynamic light scattering of the dissolved residues reveal that this growth is not totally specific.

Introduction

Semiconductor cluster molecules that are composed of a defined number of atoms are of particular interest for investigations concerning the variation of properties related to a change in size. For example, recent optical studies have shown that CdSe cluster molecules can be seen, not only with respect to their structure but also to their electronic properties, as molecular models for the bulk semiconductor.[1–4] But although a few well-defined molecular clusters formed by group 12 and 16 elements do exist, these tend to be on the smaller end of the size spectrum. Up to now the largest CdSe cluster compound that has been synthesized and characterized by single-crystal X-ray analysis contains thirty two cadmium atoms with the common formula $[Cd_{32}E_{14}(E'R)_{36}(L)_4]$ (E = Se, S; E′ = Se, S; L = neutral ligand).[5–7] Weller and coworkers found evidence from extended X-ray absorption fine structure (EXAFS) and UV/Vis[8] that the next stable cluster molecule in size is $[Cd_{54}Se_{32}(SeR)_{52}]^{8-}$, but no crystal structure from single-crystal XRD has been reported to date. It is therefore, a major goal to find new synthetic routes to enlarge the number of species in this class of materials. Most of the cluster syntheses are done in solution, but especially for one of the largest clusters $[Cd_{32}S_{14}(SC_6H_5)_{36}(DMF)_4]$, Herron et al. developed a combined solid-state/solution process in which a smaller cluster, namely $(NMe_4)_2[Cd_{10}S_4(SPh)_{16}]$, acts as a precursor for the synthesis of the larger compound.[5,9] With regard to the synthesis of 12–16 nanomaterials, Cumberland et al. have shown recently that similar smaller cluster molecules can also act in solution as convenient single-source precursors for controlled preparation of 2–9 nm CdSe and CdSe/ZnS nanocrystals.[10]

This paper reports on the investigations of the thermal properties of a series of four different M_{10}-selenide cluster molecules of the general formula $[M_{10}Se_4(SePh)_{12}(PR_3)_4]$ (M = Zn, Cd, Hg; R = organic group) by TGA. Recrystallisation of the intermediate product of the first step of the vacuum thermolysis of $[Cd_{10}Se_4(SePh)_{12}(PnPr_3)_4]$ led to the isolation of the larger cluster molecules $[Cd_{32}Se_{14}(SePh)_{36}(L)_4]$ (L = $OPPh_3$, OC_4H_8), which were characterised by single-crystal XRD.

Results and Discussion

Synthesis and Structure of the Precursor Cluster Molecules

The reaction of MCl_2 (M = Zn, Cd, Hg) with PR_3 (R = organic group), $PhSeSiMe_3$ and $Se(SiMe_3)_2$ in organic solvents results, according to Scheme 1, in the formation of crystals of $[Zn_{10}Se_4(SePh)_{12}(PnPr_2Ph)_4]$ (**1**), $[Cd_{10}Se_4(SePh)_{12}(PnPr_3)_4]$ (**2**),[1] $[Cd_{10}Se_4(SePh)_{12}(PEt_3)_4]$ (**3**, **3a**) and $[Hg_{10}Se_4(SePh)_{12}(PnPrPh_2)_4]$ (**4**).[11]

[a] Institut für Nanotechnologie (INT), Forschungszentrum Karlsruhe,
Postfach 3640, 76021 Karlsruhe, Germany
Fax: +49-7247-82-6368
E-mail: eichhoefer@int.fzk.de

$MCl_2 + PR_3$ (M = Zn, Cd, Hg)

organic solvent ↓ $PhSeSiMe_3$/ $Se(SiMe_3)_2$

$[Zn_{10}Se_4(SePh)_{12}(PnPr_2Ph)_4]$ **(1)**
$[Cd_{10}Se_4(SePh)_{12}(PnPr_3)_4]$ **(2)**
$[Cd_{10}Se_4(SePh)_{12}(PEt_3)_4]$ **(3, 3a)**
$[Hg_{10}Se_4(SePh)_{12}(PnPrPh_2)_4]$ **(4)**

Scheme 1.

Figure 1 shows, as an example, the molecular structure of a $[M_{10}Se_4(SePh)_{12}(PR_3)_4]$ (M = Zn, Cd, Hg; R = organic group) cluster core; these have been determined for all four compounds by single-crystal X-ray diffraction (Table 1). The cluster core, which comprises four adamantane cages each of which is formed by six selenium and four group 12 metal atoms, is a macrotetrahedral fragment of the sphalerite structure, which can be found in ZnSe, CdSe and HgSe. The four phosphane atoms occupy the apex positions of the resultant tetrahedron. The metal atoms are all four coordinate with distorted tetrahedral coordination geometry. Whilst most of them are bonded to either μ_3-Se^{2-}- or μ_2-$SePh^-$ ligands, those at the apex positions are also coordinated to phosphorus atoms. Mean interatomic distances vary in **1–4** because of the increasing covalent radii of zinc, cadmium and mercury (Table 2). The solution absorption spectrum for cluster **1** in THF features one maximum in the UV region at 246 nm ($\varepsilon = 2.9 \cdot 10^5\ M^{-1}\,cm^{-1}$).

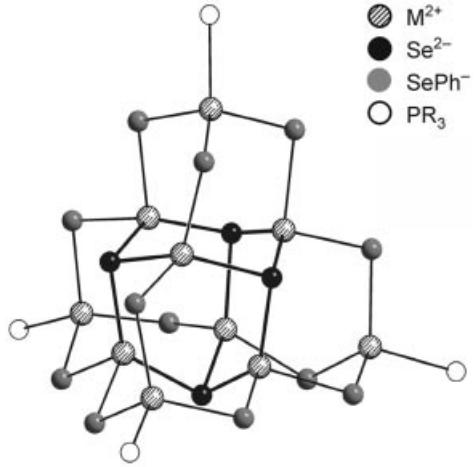

Figure 1. The $M_{10}Se_{16}P_4$ cluster core as a section of the molecular structures of $[M_{10}Se_4(SePh)_{12}(PR_3)_4]$; M = Zn (**1**), Cd (**2**, **3**, **3a**), Hg (**4**); R = organic group.

Thermogravimetric Analysis

The decomposition of **1–4** upon heating was followed by combined thermogravimetric analysis (TGA) and mass spectrometry (Figure 2). In the DTG, the mass change of **1** shows one sharp feature at 204 °C immediately followed by two further steps at 262 °C and 334 °C. The weight change in the first step corresponds to the cleavage of four $PPhnPr_2$ (calcd. 21.5%), while the added mass loss of the second and third step is equivalent to six $SePh_2$ (calcd. 38.7%) leading to the formation of ZnSe. A powder diffraction pattern proves the cubic structure of the formed material.

Thermogravimetric analysis of **2** in vacuo shows that the thermal decomposition occurs in two successive steps represented by two well-resolved peaks in the DTG curve (Figure 2). While the peak at 175 °C displays only one maximum, the other is split into two closely neighbouring maxima at 282 °C and 308 °C. The mass change of the first reaction corresponds to 16.9% which is equivalent in mass to four $PnPr_3$ (calcd. 16.2%) and some additional toluene incorporated in the crystal lattice. The intermediate product '$Cd_{10}Se_4(SePh)_{12}$' then undergoes a second reaction, beginning at around 220 °C. The mass loss is equivalent to six $SePh_2$ (calcd. 35.4%), leaving a solid residue with the formula CdSe. X-ray diffraction indicates that this solid is phase-pure CdSe in the zincblende structure. This interpretation is in good agreement with simultaneously recorded mass spectra. Starting from 40 °C, two peaks at *m/e* = 91, 92 evolve, which indicate small amounts of remaining toluene in the crystal powder. The principal product of the low-temperature weight loss event is identified to be $PnPr_3$ (*m/e* = 161, 133, 104/105, 91, 77, 62, 41, 27). The highest peaks in mass in the spectra of the second step are located between *m/e* = 150–161 and can be assigned to $(C_6H_5)_2$ (*m/e* = 154), HSePh (*m/e* = 158) and 'SePh' as a fragmentation product of $SePh_2$, although molecular peaks (*m/e* = 234; 312) of this latter compound were not detected. Therefore, the volatile products of the second step of the vacuum thermolysis of **5** were collected in a cool trap and investigated by GC-MS as a solution in THF. $SePh_2$ was found to be the main product accompanied by HSePh, $(C_6H_5)_2$ and PhSe–SePh, all with lower concentrations by approximately one-tenth.

Nearly the same decomposition sequence is observed for **3**; the second step that corresponds to the cleavage of six $SePh_2$ (calcd. 36.96%) is quite similar to that of **2** (Figure 2). However, the differential peak for the first event in the TGA of **3** appears to be much broader than that of **2** with an indicated splitting into two subprocesses. As a consequence the mean temperature for the cleavage of four PEt_3 (calcd. 12.49%) is found to be by approximately 30 °C higher than that of $PnPr_3$ in **2**. Therefore, the two steps of the thermolysis of **3** are not as well separated as for **2**. Accordingly the measured weight loss in the mass spectra indicate that PEt_3 (*m/e* = 118) and 'SePh' (*m/e* = 157) are the main decomposition products of either step 1 (low temperature) and step 2 (high temperature).

The investigations of the thermal properties of **4** reveal that it decomposes rapidly in a two-step process between 40 °C and 140 °C to yield a black residue of 12% in mass of the starting cluster with C: 0.61% and H: 0.04% (Figure 2). Powder X-ray diffraction analysis shows it to be HgSe in its cubic form, which then further decomposes at a mean

Table 1. Crystallographic Data for $[Zn_{10}Se_4(SePh)_{12}(PPhnPr_2)_4]$ (**1**), $[Cd_{10}Se_4(SePh)_{12}(PEt_3)_4]$ (**3**, **3a**), $[Cd_{32}Se_{14}(SePh)_{36}(C_4H_8O)_4]$ (**5**) and $[Cd_{32}Se_{14}(SePh)_{36}(OPPh_3)_4]$ (**6**).

	1·5C_6H_6	**3**	**3a**	**5**	**6**·9.5C_4H_8O
Formula mass	4009.77	3785.16	3785.16	10608.82	11830.05
Crystal system	triclinic	trigonal	tetragonal	trigonal	monoclinic
Space group	$P\bar{1}$	$R\bar{3}c$	$P\bar{4}$	$R\bar{3}c$	$C2/c$
a [pm]	1870.6(4)	5103.5(7)	2694.3(4)	2317.6(3)	2504.1(5)
b [pm]	1999.3(4)				4436.5(9)
c [pm]	2439.6(5)	3156.9(6)	1629.0(3)	22119(4)	3514.8(7)
α [°]	69.14(3)				
β [°]	68.54(3)				91.43(3)
γ [°]	85.77(3)				
V [10^6pm^3]	7919(3)	71209(20)	11825(3)	102888	39036(14)
Z	2	24	4	12	4
T [K]	190	190	190	190	160
$d_{calcd.}$ [g cm^{-3}]	1.682	2.118	2.126	2.055	2.013
μ(Mo-K_α) [mm^{-1}]	5.249	6.754	6.778	7.280	6.424
F[000]	3940	42700	7120	58464	22064
$2\Theta_{max}$ [°]	50	48	50	40	48
Measured reflections	39100	39426	38771	47186	66696
Unique reflections	25167	18859	20626	10616	26715
R_{int}	0.0771	0.0574	0.0477	0.0815	0.0901
Reflections with $I > 2\sigma(I)$	17284	14249	13333	8174	15726
Refined parameters	887	873	672	577	1053
$R1[I > 2\sigma(I)]$[a]	0.0753	0.0450	0.0503	0.0932	0.0660
$wR2$(all data)[b]	0.2052	0.1272	0.1420	0.2935	0.2037
Abs. struct. param.		–0.008(9)	0.474(9)		

[a] $R1 = \Sigma||F_o| - |F_c||/\Sigma|F_o|$. [b] $wR2 = \{\Sigma[w(F_o^2 - F_c^2)^2]/\Sigma[w(F_o^2)^2]\}^{1/2}$.

Table 2. Selected ranges of interatomic distances [pm] for $[Zn_{10}Se_4(SePh)_{12}(PnPr_2Ph)_4]$ (**1**), $[Cd_{10}Se_4(SePh)_{12}(PnPr_3)_4]$ (**2**) $[Cd_{10}Se_4(SePh)_{12}(PEt_3)_4]$ (**3**, **3a**) and $[Hg_{10}Se_4(SePh)_{12}(PnPrPh_2)]$ (**4**).

	1 (M = Zn)	**2** (M = Cd)	**3** (M = Cd)	**3a** (M = Cd)	**4** (M = Hg)
M–μ_3-Se	240.1–244.0(2)	257.8–259.9(1)	257.6–262.2(2)	257.0–261.2(2)	256.0–262.8(1)
M–μ_2-SePh	244.6–254.6(2)	263.1–271.6(1)	262.3–274.3(2)	263.3–274.1(2)	262.1–277.7(1)
M–P	241.3–243.4(4)	260.6(2)	257.2–261.2(6)	259.4–261.4(4)	257.5(3)
P–P	1164.6–1188.9	1246.0–1258.3	1226.6–1309.4	1229.3–1296.9	1221.4–1293.4

temperature of 226 °C; this is in rough agreement with the reported value for the beginning of the sublimation of HgSe in an evacuated quartz crucible at 226 °C.[12] However, the observed mass changes in the three-step TGA of **4** cannot be simply assigned to the cleavage of a certain amount of product like in **1–3**, as a theoretical cleavage of four PPh_2nPr (calcd. 17.88%) and six $SePh_2$ (calcd. 27.4%) should yield a residue of 54.72 mass-% of HgSe. Similar to observations of Corrigan et al. on the TGA of $[Hg_{15}Cu_{20}S_{25}(PnPr_3)_{18}]$,[13] we assume that more complex redox processes including the reduction of Hg^{2+} may take place during the thermal treatment of **4**. For the first step, the recorded mass spectra only display the peaks associated to the fragmentation products of PPh_2nPr (m/e = 152 = PPh*n*Pr and 108 = PPh). Starting with the second step, a group of peaks between m/e = 150 and 161 evolves, which is indicative of the cleavage of SePh groups. Any other products could not be clearly identified in the mass spectra.

Characterization of the Intermediate '$Cd_{10}Se_4(SePh)_{12}$'

Bulk samples of the yellow '$Cd_{10}Se_4(SePh)_{12}$' were prepared according to Scheme 2 in a porcelain boat inside a glass tube, connected to a high vacuum pump.

The X-ray powder pattern of the yellow crude powder (Figure 3) shows one strong peak at d = 1.78 nm in the low 2θ range, and three further broad and weaker peaks at higher angles (25.4°, 43.3°), the latter of which has a distinct shoulder at 47.8°. The pattern of the three weaker peaks can be successfully fitted on the basis of the cubic bulk structure of CdSe, and the broad peaks indicating the small sizes of the crystallites. An estimation of the particle size on the basis of the Scherrer equation[14] yields a mean diameter of 1.5 nm, which suggests a growth of the originally 0.7-nm sized CdSe cluster cores in **2** (size is taken as the distance of the cadmium atom at one vertex to the opposite tetrahedral face; see Figure 1). The peak at d = 1.78 nm depicts some long-range order in the powder, which most probably originates from the nanostructuring of the material.

Yellow '$Cd_{10}Se_4(SePh)_{12}$' dissolves fairly well in THF, whilst the solubility is enhanced upon addition of aliquots of tertiary phosphanes. By comparison of the UV/Vis spectra of **2** and '$Cd_{10}Se_4(SePh)_{12}$' in THF it can clearly be seen that the absorption features of **2** have changed upon thermal treatment (Figure 4a). While the characteristic peaks for **2** at 297 nm and 316 nm have disappeared, new, weakly resolved absorption maxima are detected at higher wave-

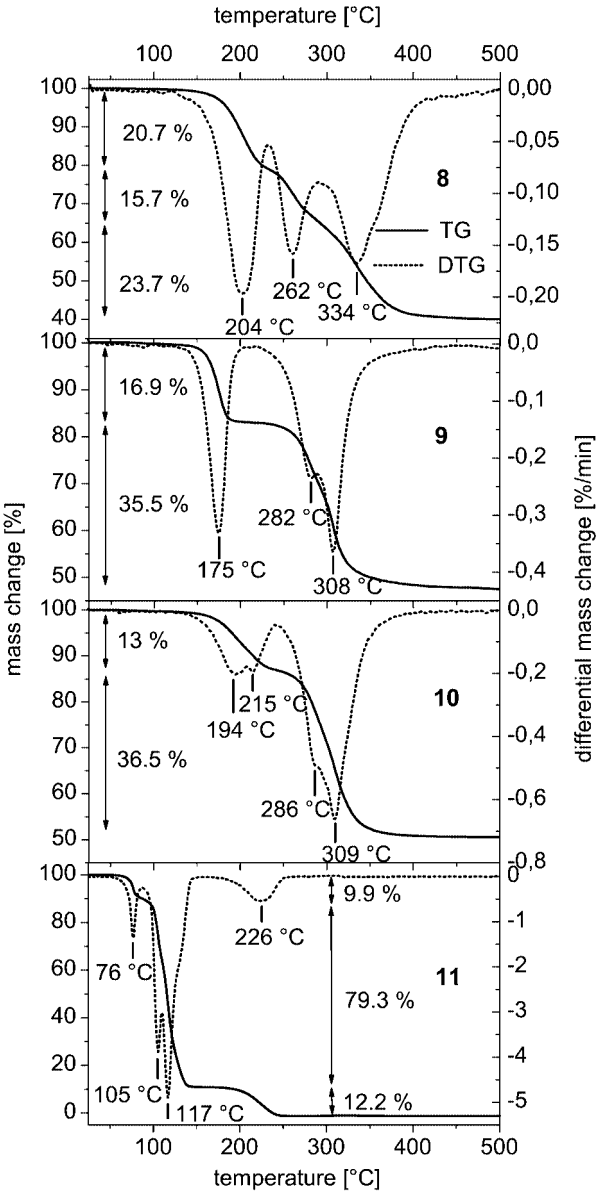

Figure 2. Thermogravimetric analysis of $[Zn_{10}Se_4(SePh)_{12}(PnPr_2Ph)_4]$ (**1**), $[Cd_{10}Se_4(SePh)_{12}(PnPr_3)_4]$ (**2**), $[Cd_{10}Se_4(SePh)_{12}(PEt_3)_4]$ (**3**, **3a**) and $[Hg_{10}Se_4(SePh)_{12}(PnPrPh_2)]$ (**4**) (straight lines). The corresponding differential thermogravimetric curves are drawn as dashed lines.

$$[Cd_{10}Se_4(SePh)_{12}(PnPr_3)_4] \quad (\mathbf{2})$$

$$\Delta / 210\ ^\circ C \;\Big|\; -4\ PnPr_3$$

$$\downarrow$$

$$`Cd_{10}Se_4(SePh)_{12}'$$

Scheme 2.

lengths suggesting a growth of the original CdSe cluster cores of **2**, which is in agreement with the particle sizes derived from powder X-ray data.

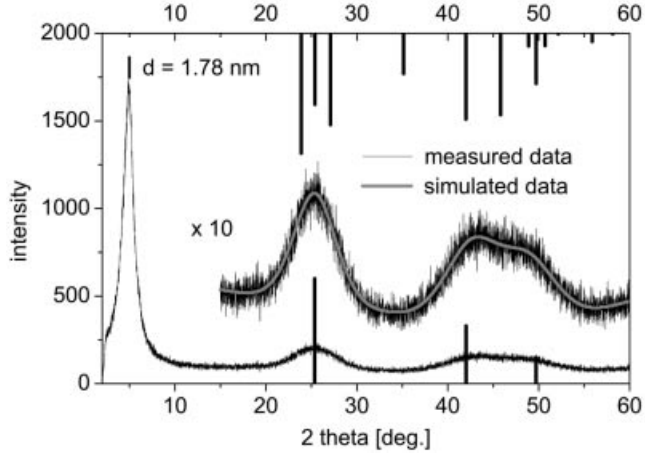

Figure 3. Powder XRD pattern for the intermediate product '$Cd_{10}Se_4(SePh)_{12}$' formed by TGA of $[Cd_{10}Se_4(SePh)_{12}(PnPr_3)_4]$ (**2**). The solid line represents a fit to the experimental data based on the peaks of cubic CdSe. Also shown are the peak patterns of cubic (downward sticks) and hexagonal (upward sticks up) CdSe.

Similar observations are made in a dynamic light scattering experiment (Figure 4b). For solutions of '$Cd_{10}Se_4(SePh)_{12}$' in THF, a broad peak for the hydrodynamic radius (resulting from the fit of the autocorrelation function) is observed, which is shifted by 0.7 nm relative to that of the precursor cluster **2** (the total diameter of **2** is estimated from a space-filling model to be 2.2 nm).[15] The increased width of the peak for the '$Cd_{10}Se_4(SePh)_{12}$' solutions results from a distribution of particle sizes, which is in agreement with the detection of several weakly resolved maxima in the UV/Vis spectrum. The shift of the peak maxima however supports the suggested growth of the '$Cd_{10}Se_4(SePh)_{12}$' cluster cores of **2** during thermal treatment.

Synthesis and Structure of $[Cd_{32}Se_{14}(SePh)_{36}(L)_4]$; L = OC_4H_8 (5), $OPPh_3$ (6)

Dissolution of the crude yellow powder resulting from the thermal treatment of **2** with the formal composition '$Cd_{10}Se_4(SePh)_{12}$' in THF yields pale yellow crystals after one night. Although some of these crystals appear to be perfect, they diffract only up to 25° in 2θ, and the determination of a hexagonal cell was only possible on the basis of 60% of the reflections being indexed ($a = b = 3929.1$, $c = 3017.1$ pm). Additionally, one axis shows a superstructure splitting of the reflections, which altogether makes a solution of the structure impossible. The separation of the supernatant solution from the crystals and subsequent concentration by evaporation of more than half of the solvent yielded other more suitable crystals for X-ray analysis, with the composition $[Cd_{32}Se_{14}(SePh)_{36}(OC_4H_8)_4]$ (**5**) (Scheme 3). Immediate addition of six equiv. triphenylphosphineoxide during the dissolution of '$Cd_{10}Se_4SePh_{12}$' inTHF avoided the formation of the initially formed weak diffracting crystals. Instead, pale yellow pinlike crystals of $[Cd_{32}Se_{14}(SePh)_{36}(OPPh_3)_4]$ (**6**) grew upon indirect layering of the solution with acetone (Scheme 3). However, the theo-

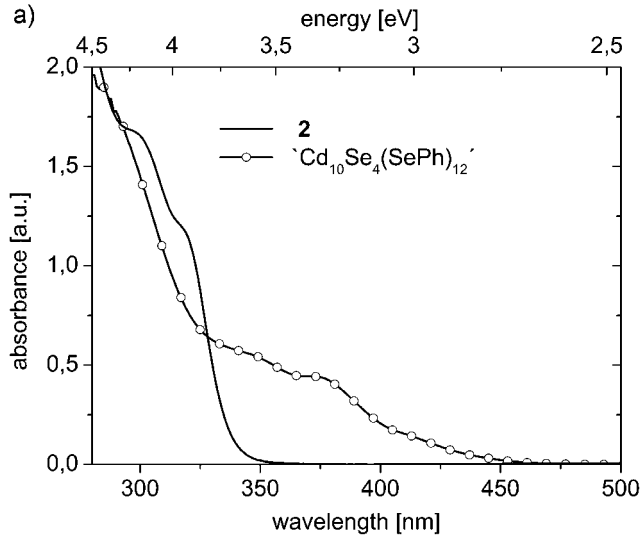

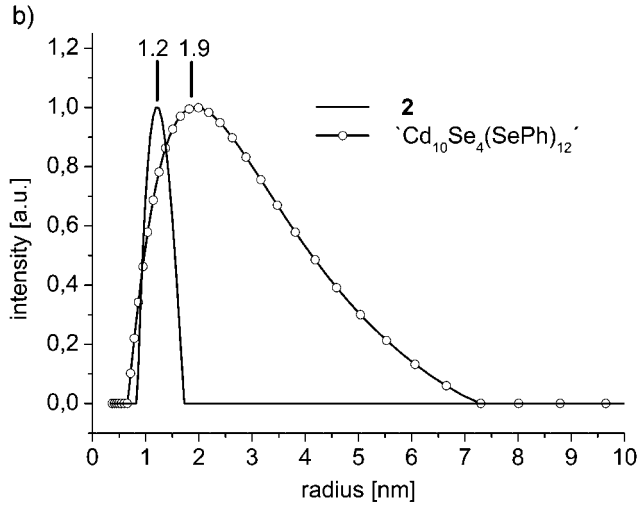

Figure 4. a) UV/Vis spectra of $[Cd_{10}Se_4(SePh)_{12}(PnPr_3)_4]$ (**2**) and the intermediate product '$Cd_{10}Se_4(SePh)_{12}$' of the TGA of **2** in THF; b) resulting peaks for the hydrodynamic radii of **2** and '$Cd_{10}Se_4(SePh)_{12}$' in THF from the fit of the autocorrelation function.

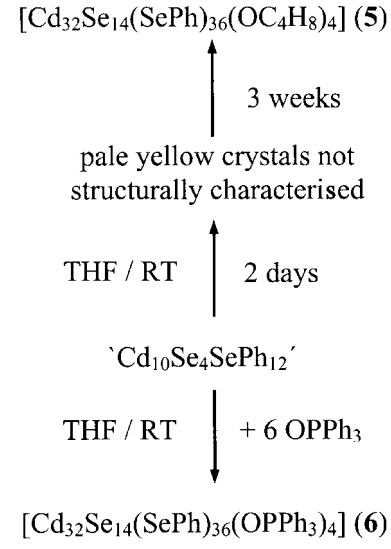

Scheme 3.

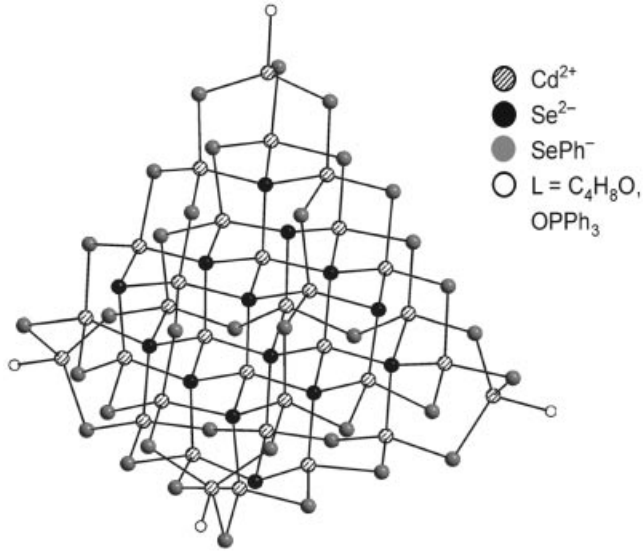

Figure 5. The $Cd_{32}Se_{50}O_4$ cluster core as a section of the molecular structures of $[Cd_{32}Se_{14}(SePh)_{36}(OC_4H_8)_4]$ (**5**) and $[Cd_{32}Se_{14}(SePh)_{36}(OPPh_3)_4]$ (**6**).

retical stoichiometric formation of **5** and **6** from '$Cd_{10}Se_4SePh_{12}$' produces a slight excess of cadmium atoms and phenylselenolate ligands with respect to the composition of the precursor compound, which suggests the formation of unidentified by-products in the reaction as represented by the unknown crystals (see also discussion of powder XRD and UV/Vis below).

Both compounds, **5** which crystallises in the space group $R\bar{3}c$ and **6** which crystallises in $C2/c$, exhibit the same tetrahedral cluster core structure $[Cd_{32}Se_{14}(SePh)_{36}L_4]$, with either C_4H_8O (**5**) or $OPPh_3$ (**6**) at the apex positions (Figure 5). This cluster framework is built up of 13-fused CdSe adamantane cages with four barrelene CdSe cages at each of the corners. Adamantane cages are the building blocks of the cubic zincblende structure of CdSe, while barrelene cages are those of the hexagonal wurtzite type. Thus, it is similar to the known M_{32} chalcogenide cluster molecules such as $[Cd_{32}S_{14}(SPh)_{36}(DMF)_4]$ (DMF = *N*,*N*-dimethylformamide),[5] $[Cd_{32}S_{14}(SCH_2CH(OH)CH_3)_{36}(H_2O)_4]$[6] and $[Hg_{32}Se_{14}(SePh)_{36}]$,[7] but slightly different to the closely related cluster $[Cd_{32}Se_{14}(SePh)_{36}(PPh_3)_4]$[7] and distinctly dif-ferent to a recently characterized cluster of composition $[Hg_{34}Te_{16}(SePh)_{36}(PPhnPr_2)_4]$.[16] The difference in structure in relative to that found in **5** and **6** (Figure 6) lies with the build up of the CdSe framework. A rotation of a corner part of the structure in **5** or **6** that consists of one barrelene cage and three adamantane cages by 120° (around the threefold axis pointing from this corner to the opposite triangular face) converts these three adamantane cages into three barrelene cages and thus leads to the structure of

$[Cd_{32}Se_{14}(SePh)_{36}(PPh_3)_4]$ without changing the stoichiometry and the overall charge of the cluster. This cluster therefore comprises an increased number of seven barrelene cages and only ten adamantane cages in comparison to the numbers found in **5** and **6**. In principle this twisting should be possible at all four corners of the '$Cd_{32}Se_{14}(SePh)_{36}$' cluster core, which would result in a build up of one adamantane cage and 16 barrelene cages, a structure which has not yet been synthesized and characterized. The problems in crystallizing these compounds are maybe due to this geometric isomerism which reflects the dimorphism of bulk CdSe, together with a huge theoretical amount of isomeric-structures caused by the two possible positions for the phenyl groups of each μ_2-SePh$^-$ ligand.[17] Another tetrahedral cluster composed of elements of group 12 and 16 with a closely related composition and size but different structure is $[Hg_{34}Te_{16}(SePh)_{36}(PPhnPr_2)_4]$.[16] The '$Hg_{34}Te_{16}Se_{36}$' cluster core is completely formed by 20 adamantane cages and can be considered as an idealized fragment of the cubic sphalerite lattice, but with a mercury vacancy in the centre. Although the cluster cores of **5** and **6** are also formed by adamantane cages, except the barrelane cages at the four corners, both structures differ in their geometric centres. Whilst at the centre of $[Hg_{34}Te_{16}(SePh)_{36}(PPhnPr_2)_4]$, there is a mercury vacancy on what should be a formal atomposition, the centre of **5** and **6** lies within the centre of theinner adamantane cage and thus on a tetrahedral hole. This situation shows, in principle, the two possibilities of nucleation of a CdSe crystal, one where it grows regularly on all sides from a preformed 'Cd_4Se_6' adamantane cage and the other from a tetrahedral '$HgTe_4$' unit. The CdSe bond distances for **5** and **6** listed in Table 3 display slightly different ranges for the different bridging modes of the selenium ligands, either μ_4-Se^{2-}, μ_3-Se^{2-} or μ_2-Se^-, which are in analogy to those ranges found in the similar cluster, $[Cd_{32}Se_{14}(SePh)_{36}(PPh_3)_4]$.[7]

A comparison of the measured and calculated X-ray powder diffraction patterns for **5** and **6** reveal their reason-

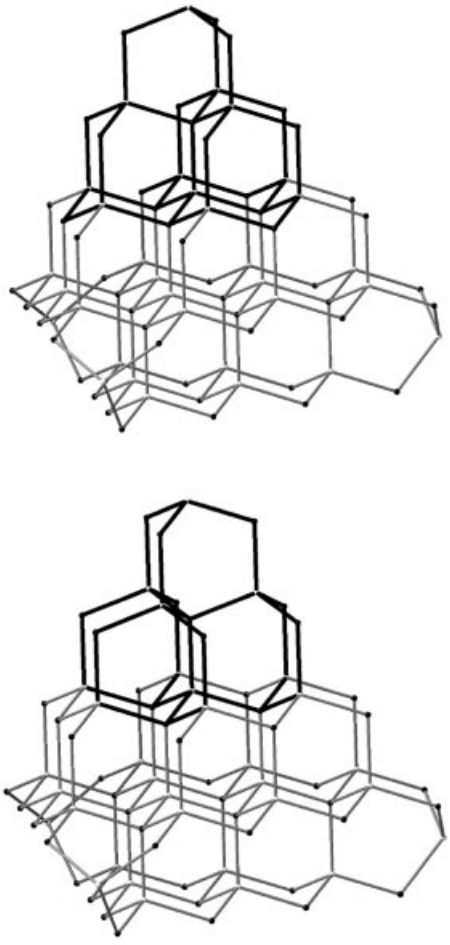

Figure 6. Schematic drawing of the different build up of the $Cd_{32}Se_{50}$ cluster cores in $[Cd_{32}Se_{14}(SePh)_{36}(OC_4H_8)_4]$ (**5**), $[Cd_{32}Se_{14}(SePh)_{36}(OPPh_3)_4]$ (**6**) (above) and $[Cd_{32}Se_{14}(SePh)_{36}(PPh_3)_4]$[7] (below) with the differing part highlighted in black.

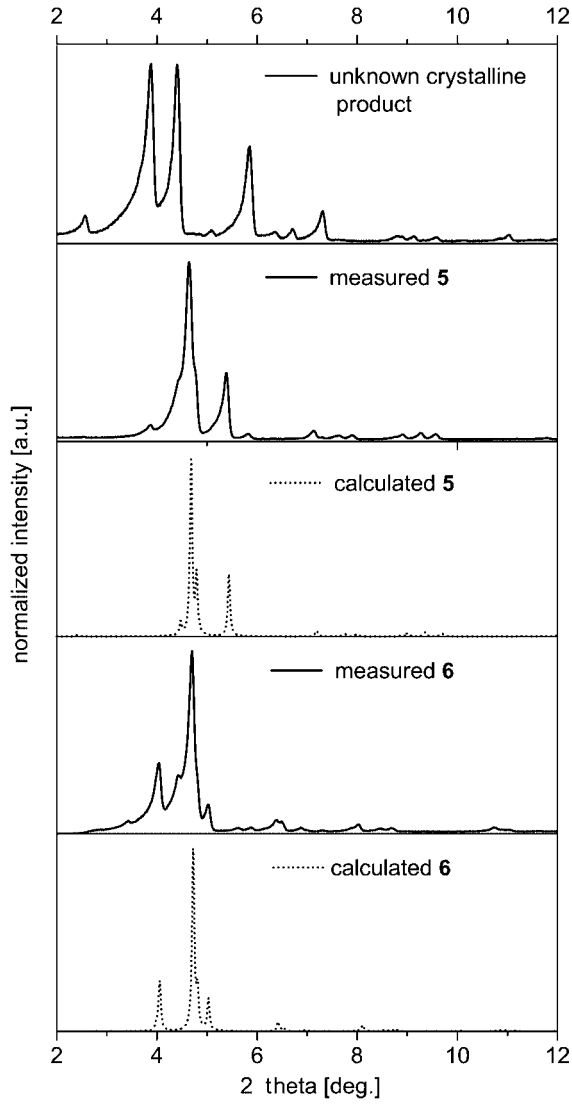

Figure 7. Measured (straight line) and calculated (dotted line) X-ray powder patterns for $[Cd_{32}Se_{14}(SePh)_{36}(OC_4H_8)_4]$ (**5**) and $[Cd_{32}Se_{14}(SePh)_{36}(OPPh_3)_4]$ (**6**) which can be compared to the pattern of the unknown crystalline preproduct resulting from the recrystallisation of the intermediate product '$Cd_{10}Se_4(SePh)_{12}$' of the TGA of $[Cd_{10}Se_4(SePh)_{12}(PnPr_3)_4]$ (**2**) (Scheme 3).

Table 3. Selected ranges and mean values for bond distances [pm] for $[Cd_{32}Se_{14}(SePh)_{36}(OC_4H_8)_4]$ (**5**) and $[Cd_{32}Se_{14}(SePh)_{36}(OPPh_3)_4]$ (**6**).

Bond	No. of bonds	**5**		**6**	
		Range	Mean value	Range	Mean value
μ_4-Se^{2-}–Cd	40	261.8–267.4(3)	264.6	261.7–266.6(2)	264.0
μ_3-Se^{2-}–Cd	12	257.6–259.1(3)	258.0	257.5–258.7(2)	258.3
μ_2-$SePh^-$–Cd	72	258.2–269.9(4)	264.4	260.0–270.1(2)	265.1
O–Cd	4	236.7–237.7(30)	237.5	222.7–225.9(11)	224.3

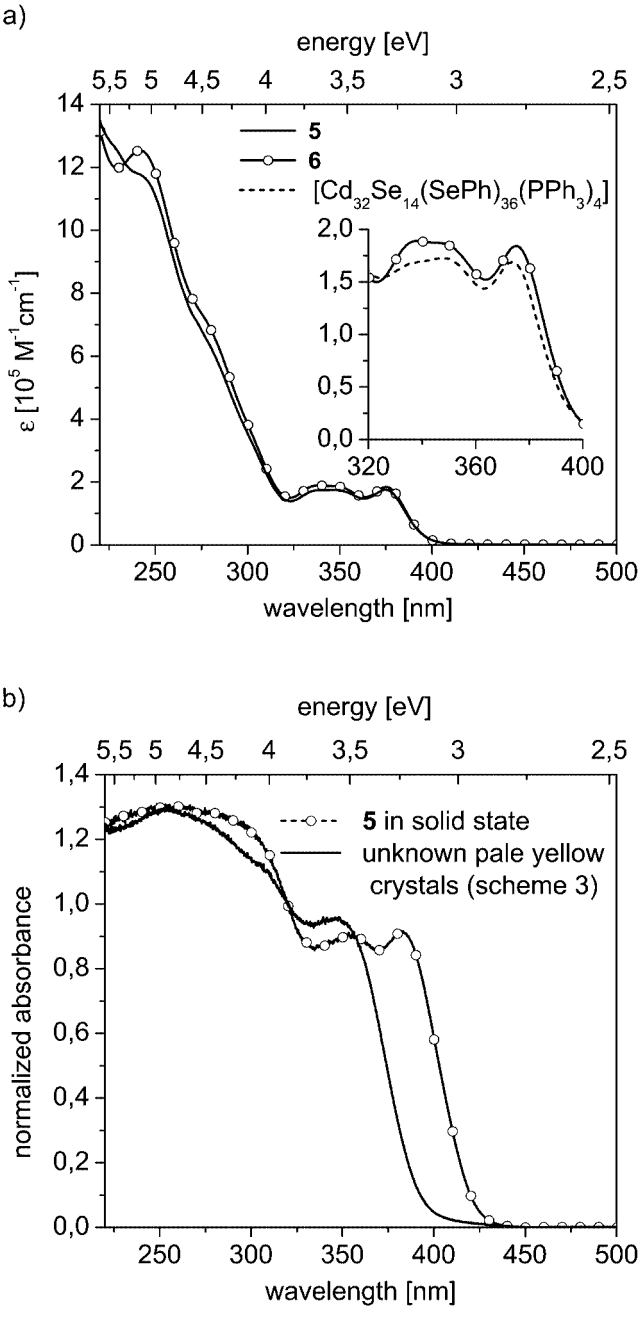

Figure 8. a) UV/Vis spectra of $[Cd_{32}Se_{14}(SePh)_{36}(OC_4H_8)_4]$ (**5**) and $[Cd_{32}Se_{14}(SePh)_{36}(OPPh_3)_4]$ (**6**) in THF. The inset displays a magnification of the absorption bands of **5** between 320 and 400 nm relative to the bands of the very similar cluster $[Cd_{32}Se_{14}(SePh)_{36}(PPh_3)_4]$; b) UV/Vis spectra of **5** and the unknown pale yellow crystals (see Scheme 3) in solid state.

able crystalline purity with respect to the formation of a mixture of compounds (Figure 7), although weak additional reflections in the patterns of **5** and **6** indicate cocrystallisation of small amounts of an unknown crystalline product in both compounds. However, the location of the strong reflections in the powder pattern of these unknown crystals at low 2θ values reflect long-range ordering in a size range comparable to **5** and **6**.

The UV/Vis spectra in THF (Figure 8a) are quite similar for **5** and **6**. Starting from higher wavelengths, the first absorption maximum is observed at 375 nm (3.3 eV) [the extinction coefficient for **5** in THF is $1.84 \cdot 10^5$ $M^{-1}cm^{-1}$ and for **6**, $1.76 \cdot 10^5$ $M^{-1}cm^{-1}$] followed by a broad peak centred at 343 nm (3.6 eV) which most probably consists of two closely neighbouring transitions at either 338 nm (3.7 eV) and 348 nm (3.6 eV). The following increase in absorbance in the region from 321 nm to 210 nm indicates further weakly resolved maxima and shows a last peak for **5** at 241 nm (5.12 eV) and a related shoulder for **6** at a similar position. The inset in Figure 8a displays a comparison of the spectra of **5** and the very similar cluster $[Cd_{32}Se_{14}(SePh)_{36}(PPh_3)_4]$, which has a slightly shifted first absorption maximum at 373 nm. In contrast to **5**, the unknown crystalline pale yellow product according to Scheme 3 is mostly insoluble in THF. The solid-state UV/Vis spectrum in Figure 8b shows the lowest energy absorption peak at 346 nm (3.58 eV), while under similar conditions, the spectrum for **5** shows the first maximum at 383 nm (3.24 eV). Therefore, the position of the lowest-energy transition between that of **2** and **5** points to an intermediate cluster size, for example, a cluster cage with 17 cadmium atoms such as '$Cd_{17}Se_4(SePh)_{24}$', which was found in $[Cd_{17}Se_4(SePh)_{24}(PnPr_2Ph)_4]^{2+}$.[1] The low solubility suggests an ionic or polymeric species. These findings are also in agreement with the elemental analysis (C: 30.2, H: 2.1%) of the preliminary crystallizing powder, which displays higher values than those calculated for **5** (C: 26.3, H 2.0%).

Experimental Section

Synthesis

Standard Schlenk techniques were employed throughout the syntheses using a double manifold vacuum line with high purity dry nitrogen. The solvents tetrahydrofuran (THF), dimethylethyleneglycol (DME) and benzene were dried over sodium benzophenone, and toluene, over $LiAlH_4$, and distilled under nitrogen. Anhydrous $ZnCl_2$, $CdCl_2$ and $HgCl_2$ were purchased from Aldrich. $PhSeSiMe_3$[18] and $Se(SiMe_3)_2$[19] were prepared according to stan-

dard literature procedures. $Se(SinBu_3)_2$ was prepared according to the synthesis of $Se(SiMe_3)_2$ with $ClSinBu_3$ instead of $ClSiMe_3$.

1: $ZnCl_2$ (0.28 g, 2.05 mmol) was dissolved in benzene (50 mL) with the addition of $PPhnPr_2$ (0.43 mL, 2.05 mmol). $PhSeSiMe_3$ (0.55 mL, 2.87 mmol) was then added, and the resulting clear solution was stirred for 2 h. Addition of $Se(SiMe_3)_2$ (0.18 mL, 0.82 mmol) led to the formation of some droplets of colourless oil, which dissolves again upon standing for two days. Layering with *n*-pentane leads to the formation of colourless crystals of $[Zn_{10}Se_4(SePh)_{12}(PnPr_2Ph)_4]$ (**1**). Yield: 0.66 g, 80%. $C_{120}H_{136}Zn_{10}P_4Se_{16}$ (3619.45): calcd. C 39.82, H 3.79; found C 40.06, H 3.74%.

2: according to ref.[1].

3, **3a:** $CdCl_2$ (0.32 g, 1.75 mmol) was dissolved in DME (30 mL) with the addition of PEt_3 (0.64 mL, 4.36 mmol). $PhSeSiMe_3$ (0.54 mL, 2.8 mmol) was then added at 0 °C, and the resulting clear solution was stirred for 2.5 h. Addition of $Se(SiMe_3)_2$ (0.12 mL, 0.53 mmol) at 0 °C and subsequent standing at room temperature led to the formation of a mixture of colourless crystals of $[Cd_{10}Se_4(SePh)_{12}(PEt_3)_4]$ (**3**, **3a**). Yield: 0.50 g, 76%. $C_{96}H_{120}Cd_{10}P_4Se_{16}$ (3785.36): calcd. C 30.46, H 3.20; found C 30.43, H 3.31%.

4: according to ref.[11].

'$Cd_{10}Se_4(SePh)_{12}$': Bulk samples of the intermediate '$Cd_{10}Se_4(SePh)_{12}$', identified from the TGA experiments, were prepared by heating **2** in a porcelain boat inside a glass tube connected to a high vacuum pump via a cool trap. Samples of **2** (up to 0.5 g) were heated at 3 °C/min to 210 °C and then immediately cooled down by opening of the oven. The originally white/colourless crystals changed to give an intense-coloured yellow powder. $C_{72}H_{60}Cd_{10}Se_{16}$ (3312.73): calcd. C 26.11, H 1.82; found C 26.01, H 1.87%.

5: '$Cd_{10}Se_4(SePh)_{12}$' (0.043 g, 0.013 mmol) was dissolved in THF (12 mL). Hexagonal shaped crystals of poor diffraction quality were obtained after overnight standing. After two days the clear supernatant solution was separated from the crystals and this flask connected to another flask which contains Diglyme (50 mL). Slow evaporation of more than half of the THF solution into the Diglyme solution over a period of 3 weeks yielded pale yellow crystals of $[Cd_{32}Se_{14}(SePh)_{36}(C_4H_8O)_4]$ (**5**) as well as small amounts of the hexagonal ones with unknown composition. Yield: 0.018 g, 45% calculated for reaction of 3.5 equiv. '$Cd_{10}Se_4(SePh)_{12}$' to yield 1 equiv. **5**, according to Scheme 3. $C_{232}H_{212}Cd_{32}O_4Se_{50}$ (10609.35): calcd. C 26.27, H 2.01; found C 26.11, H 2.02%.

6: '$Cd_{10}Se_4(SePh)_{12}$' (0.097 g, 0.0293 mmol) was dissolved in THF (10 mL). Then $OPPh_3$ (1.21 mL of a 0.176 M solution in THF) was added and layered with acetone through slow diffusion by evaporation via a connected flask to give pale yellow crystals of $[Cd_{32}Se_{14}(SePh)_{36}(OPPh_3)_4]$ (**6**). Yield: 0.048 mg, 50% calculated for reaction of 3.5 equiv. '$Cd_{10}Se_4(SePh)_{12}$' to yield 1 equiv. **6** according to Scheme 3. $C_{288}H_{240}Cd_{32}O_4P_4Se_{50}$ (11434.09): calcd. C 30.25, H 2.12; found C 29.95, H 2.09%.

Crystallography

Crystals suitable for single-crystal X-ray diffraction were taken directly from the reaction solutions of the compounds and then selected in perfluoroalkylether oil.

Single-crystal X-ray diffraction data were collected with the use of graphite-monochromatised Mo-K_α radiation (λ = 0.71073 Å) on a STOE IPDS II (Imaging Plate Diffraction System) equipped with a Schneider rotating anode. The structures were solved with the direct methods program SHELXS[20] of the SHELXTL PC suite programs, and were refined with the use of the full-matrix least-squares program SHELXL.[20] Molecular diagrams were prepared by using the program SCHAKAL 97[21] and DIAMOND.[22]

All Zn, Cd, Se and P atoms were refined with anisotropic displacement parameters, whilst all C and O atoms were refined isotropically with the exception of **6** where the O atoms were treated anisotropically. Some of the phenyl rings were refined with a model of disorder **1**: C43–C48 and C103–C108, **3a**: C43–C48 and C91–C96, **5**: C1–C6 and C55–C60. The phenyl group C67–C72 in **5** could only be refined as a rigid group with half occupancy. One THF ligand (O2, C77, C78) in **5**, which coordinates to Cd2 at one apex position of the cluster core resides on a threefold axis. It was refined as a threefold degenerate solvent molecule but could also in general indicate a twinning of the crystals. Only two of the solvent THF molecules in **6** were refined with half occupancy. Residual electron density in the difference Fourier map of **1**, **5** and **6** indicates the existence of additional disordered solvent molecules in the crystal lattice that could not be refined successfully. Problems in the X-ray structural analysis of **5** arise from the very long *c* axis of the unit cell. In order to avoid an overlapping of reflections, a maximum detector distance (200 mm, $2\Theta_{max}$ = 40°) was chosen during the measurement together with a small effective mosaic spread and a small reflection box in the integration.

CCDC-250987 (**1**), CCDC-250988 (**3**), CCDC-250989 (**3a**), CCDC-250990 (**5**) and CCDC-250991 (**6**) contain the supplementary crystallographic data for this paper. These data can be obtained free of charge from The Cambridge Crystallographic Data Centre via www.ccdc.cam.ac.uk/data_request/cif.

X-ray powder diffraction patterns (XRD) were measured on a STOE STADI P diffractometer (Cu-K_α radiation, Germanium monochromator, Debye–Scherrer geometry) in sealed glass capillaries. Theoretical powder diffraction patterns for **1** and **2** were calculated on the basis of the atom coordinates obtained from single-crystal X-ray analysis by using the program package STOE WinXPOW.[23]

Physical Measurements

UV/Vis absorption spectra of cluster molecules in solution were measured on a Varian Cary 500 spectrophotometer in quartz cuvettes. Solid-state spectra were measured as micron-sized crystalline powders in mineral oil between quartz plates with a Labsphere integrating sphere.

Light scattering experiments were carried out with an ALV-NIBS particle sizer. The time correlation functions were measured with an ALV-5000/E Multiple Tau Digital Correlator. The light source a 3 mW He/Ne-Laser (632.8 nm) is therein combined with a focusing optic and a highly sensitive single photon detector in back-scattering geometry. All of the measurements were carried out at a temperature of 25 °C ± 0.1 °C in quartz cuvettes sealed with a septum to avoid decontamination of the samples with oxygen and water.

Thermogravimetric analyses were run on a thermobalance STA 409 from Netzsch in vacuo (heating rate 2 K/min). The balance was coupled with a quadrupole mass spectrometer QMG 422 from Balzers.

GC-MS spectra were performed on an Agilent Technologies 6869N Network GC System equipped with an Agilent 5973 Network Mass Selective Detector using 30 m DB5 columns.

Acknowledgments

This work was supported by the Deutsch-Israelisches Programm (DIP) and the Deutsche Forschungsgemeinschaft (centre for func-

tional nanostructures CFN). The author is grateful to Prof. Dr. D. Fenske for helpful discussions and for providing excellent working conditions, E. Tröster for her invaluable assistance in the practical work, Dr. P. Scheer for running the TGA and Dr. Dale Cave for careful revision of the manuscript.

[1] V. Soloviev, A. Eichhöfer, D. Fenske, U. Banin, *J. Am. Chem. Soc.* **2000**, *122*, 2673–2674.
[2] V. Soloviev, A. Eichhöfer, D. Fenske, U. Banin; *J. Am. Chem. Soc.* **2001**, *123*, 2354–2364.
[3] A. Eichhöfer, A. Aharoni, U. Banin, *Z. Anorg. Allg. Chem.* **2002**, *628*, 2415–2421.
[4] A. Aharoni, A. Eichhöfer, D. Fenske, U. Banin, *Opt. Mat.* **2003**, *24*, 43–49.
[5] N. Herron, J. C. Calabrese, W. E. Farneth, Y. Wang, *Science* **1993**, *259*, 1426–1428.
[6] T. Vossmeyer, G. Reck, L. Katsikas, E. T. K. Haupt, B. Schulz, H. Weller, *J. Am. Chem. Soc.* **1995**, *117*, 12881–12882.
[7] S. Behrens, M. Bettenhausen, A. C. Deveson, A. Eichhöfer, D. Fenske, A. Lohde, U. Woggon, *Angew. Chem.* **1996**, *108*, 2360–2363; *Angew. Chem. Int. Ed. Engl.* **1996**, *35*, 2215–2218.
[8] J. Rockenberger, L. Tröger, A. L. Rogach, M. Tischer, M. Grundmann, A. Eychmüller, H. Weller, *J. Chem. Phys.* **1998**, *108*(18), 7807–7815.
[9] W. E. Farneth, N. Herron, Y. Wang, *Chem. Mater.* **1992**, *4*, 916–922.
[10] S. L. Cumberland, K. M. Hanif, A. Javier, G. A. Khitrov, G. F. Strouse, S. M. Woessner, C. S. Yun, *Chem. Mater.* **2002**, *14*, 1576–1584.
[11] A. Eichhöfer, E. Tröster, *Eur. J. Inorg. Chem.* **2002**, 2253–2256.
[12] H. Gobrecht, U. Gerhardt, B. Peinemann, A. Tausend, *J. Appl. Phys.* **1961**, *32*, 2246–2250.
[13] D. T. T. Tran, L. M. C. Beltran, C. M. Kowalchuk, N. R. Trefiak, N. J. Taylor, J. F. Corrigan, *Inorg. Chem.* **2002**, *41*(22) 5693–5698.
[14] P. Scherrer, *Göttinger Nachrichten* **1918**, *2*, 98; H. Krischner, *Einführung in die Röntgenfeinstrukturanalyse*, 4te überarbeitete Auflage, Vieweg, Braunschweig, **1990**, 108.
[15] A. Eichhöfer, C. v. Hänisch, M. Jacobsohn, U. Banin, *Mat. Res. Soc. Symp.* **200**1, 636, D9.53.1–D9.53.9.
[16] A. Eichhöfer, P. Deglmann, *Eur. J. Inorg. Chem.* **2004**, 349–355.
[17] I. G. Dance, A. Choy, M. L. Scudder, *J. Am. Chem. Soc.* **1984**, *106*, 6285–6295.
[18] N. Miyoshi, H. Ishii, K. Kondo, S. Mui, N. Sonoda, *Synthesis* **1979**, 301–304.
[19] H. Schmidt, H. Ruf, *Z. Anorg. Allg. Chem.* **1963**, *321*, 270–273.
[20] G. M. Sheldrick, *SHELXTL PC version 5.1 An Integrated System for Solving, Refining, and Displaying Crystal Structures from Diffraction Data*, Bruker Analytical X-ray Systems, Karlsruhe, **2000**.
[21] E. Keller, *SCHAKAL 97, A Computer Program for the Graphic Representation of Molecular and Crystallographic Models*, University of Freiburg, **1997**.
[22] K. Brandenburg, *DIAMOND version 2.1d, Visual Crystal Structure Information System*, Bonn, **2000**.
[23] STOE, *WinXPOW*, STOE & Cie GmbH, Darmstadt, **2000**..

Received: September 24, 2004

